axioms

MDPI

Communication

Modulation Transfer between Microwave Beams: Angular Dependence of the Delay-Time

Ilaria Cacciari *,† and Anedio Ranfagni †

Consiglio Nazionale delle Ricerche, Istituto di Fisica Applicata "Nello Carrara", Via Madonna del Piano 10, 50019 Sesto Fiorentino, Italy
* Correspondence: i.cacciari@ifac.cnr.it
† These authors contributed equally to this work.

Abstract: Further measurements of delay time, in the transfer of modulation between microwave beams, are reported even considering the angular dependence in the orientation of the F_1 c.w. launcher. The obtained results allow for a better interpretation of the observed phenomenology on the basis of a more sophisticated analysis, which takes into account the presence of pole singularities in field-amplitude evaluations according to the saddle point method. The model already presented in one of our previous publications, consisting of a photon–photon scattering mechanism as concomitant with a stochastic process, is then confirmed.

Keywords: microwave propagation; delay-time angular dependence; saddle point method

MSC: 41A60; 30E15

Citation: Cacciari, I.; Ranfagni, A. Modulation Transfer between Microwave Beams: Angular Dependence of the Delay-Time. *Axioms* **2023**, *12*, 492. https://doi.org/10.3390/axioms12050492

Academic Editor: Valery Y. Glizer

Received: 4 April 2023
Revised: 16 May 2023
Accepted: 17 May 2023
Published: 18 May 2023

1. Introduction

The present work, which can be considered as a continuation of what is given in [1], is devoted to reporting further more accurate results, related to the delay time that occurs in the modulation transfer between microwave beams. In particular, further information about the origin of the modulation transfer event can be supplied by studying the angular dependence in the orientation of the launcher of the F_1 c.w. beam. The origin of the observed phenomenology [1] has been firstly recognized in Refs. [2,3] and explained by assuming that the nature of the process is stochastic. Indeed, the model adopted in [2], although still based on the competition of two waves, only one of which assumed modulated, while the other is c.w., hypothesized the stochastic nature of the process only as collateral aspect. On the contrary, in [3], the possibilities offered by the stochastic character were examined in two possible ways. One interpreted the delay-time as resulting from zig-zag random paths experienced by the "particle": a kind of motion that is equivalent to the telegrapher's equation [4,5]. The other way, already based on a more conventional electromagnetic approach [6]—the same is also adopted in the present work—was dependent on the stochastic nature for the presence of a dissipative parameter in Equation (3) there reported; see below Equation 1 in the present paper. Then, as in Ref. [1], the model was perfected with the combination of a photon-photon scattering mechanism. This latter was made plausible by making use of considerations of relativistic nature, which lead to a photon virtual mass sufficiently large to well support the hypothesized model.

This fact was even a consequence of the inversion of roles between "real time" and "randomized time" [4,5], this latter becoming an observable quantity as usually occurs in classically forbidden processes [1].

The present work is organized as follows. In Section 2, we briefly describe the experimental setup. In Section 3, we present new experimental results of the delay time and their preliminary interpretation. Section 4 is devoted to a more sophisticated analysis of the experimental results, and the concluding remarks are given in Section 5.

2. Experimental Method

Delay-time measurements, in the transfer of modulation between microwave beams, have been performed using the experimental setup similar to the one in Ref. [1], apart from the possibility of the orientation of the F_1 launcher. It essentially consists of two crossing microwave beams originated by the same generator at 9.3 GHz, one of which F_1 in c.w., the other F_2 modulated by a square wave at $\sim$800 Hz; the receiver was placed in front of the F_1 launcher at a variable distance ρ, and α is the tilting angle, see Figure 1.

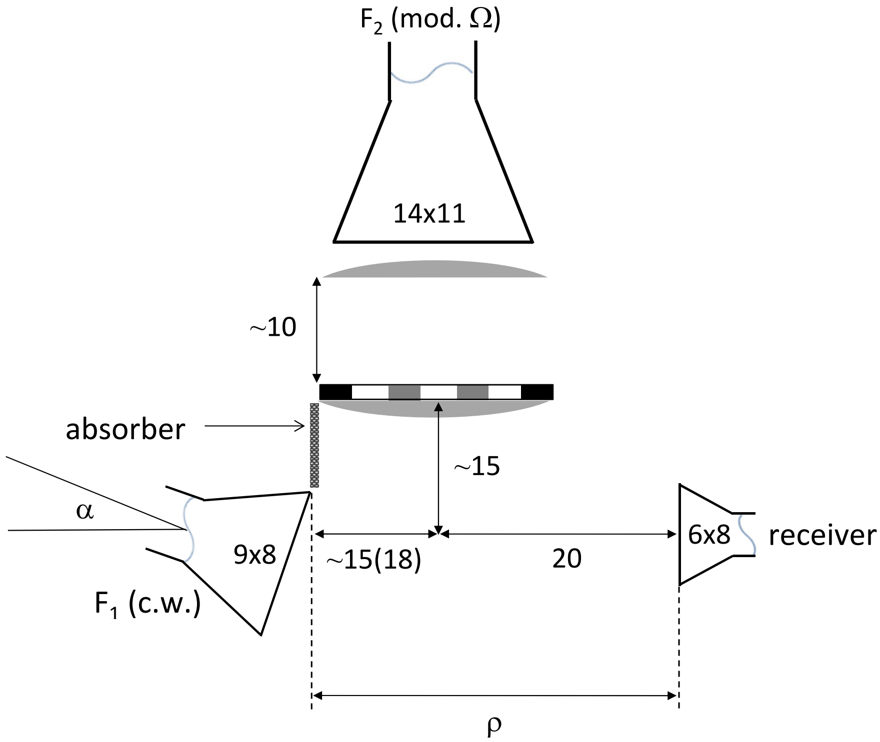

Figure 1. The experimental setup operating at 9.3 GHz. The typical geometry consisted of two horn antennas as launchers for the F_1 c.w. beam and the F_2 modulated beam, traveling through a composed pupil in order to reduce its width. The receiver horn antenna was placed at distance ρ from the F_1 launcher, where α represents its tilting angle. All the dimensions are expressed in centimeters.

3. Delay-Time Results: A Preliminary Interpretation

The measurements were performed over the rise or the fall time (of the order of nanoseconds) of the square-wave modulation. The results relative to two determinations vs. ρ (with ρ comprised between 15 and 52 cm) are reported in Figure 2; they show a rather regular oscillating behavior with a spatial periodicity of about 8 cm.

A plausible interpretation of this behavior can be given invoking a model based on the competition (interference) of two waves propagating along two directions forming an angle δ between them. According to the analysis of Ref. [6], the resulting delay can be expressed as

$$\frac{\tau_\varphi}{T} = \pm \frac{d\varphi}{d(kl)} = \pm \frac{(E_2/E_1)^2 + (E_2/E_1)\cos kl}{1 + (E_2/E_1)^2 + 2(E_2/E_1)\cos kl}, \tag{1}$$

where E_1 and E_2 are the amplitude relative to F_1 and F_2 beam, respectively. According to the assumed stochastic nature of the process [2,3], the propagation constant kl is given by $2a(\rho - \rho_i)/v$, where a is the dissipative parameter entering the telegrapher's equation [4,5], ρ_i is the initial value of ρ, and v the propagation velocity. By using $R = (E_1 + E_2)/(E_1 - E_2)$

in Equation (1), we obtain the following expression, suitable for describing the experimental data in Figure 2:

$$\tau(\rho) = A\frac{\left(\frac{R-1}{R+1}\right)^2 + \left(\frac{R-1}{R+1}\right)\cos[2a(\rho-\rho_i)/v]}{1+\left(\frac{R-1}{R+1}\right)^2 + 2\left(\frac{R-1}{R+1}\right)\cos[2a(\rho-\rho_i)/v]}e^{-\rho/\rho_0} + C_{1,2} \tag{2}$$

where $A < 0$, according to the negative determination in Equation (1), has to be considered as a fitting parameter, $e^{-\rho/\rho_0}$ accounts for the evident amplitude damping, and the constant $C_{1,2}$ for the data offset. The resulting curves obtained for parameter values such as $A = -11$ ns, $R = 3$, $\rho_i = 14$ cm, $\rho_0 = 25$ cm, $C_1 = 8$ ns, $C_2 = 3$ ns, and $a/v = 0.3925$, in order to have a spatial period of $\sim$8 cm, are depicted in Figure 1 and represent a rough but plausible description of the experimental data there reported.

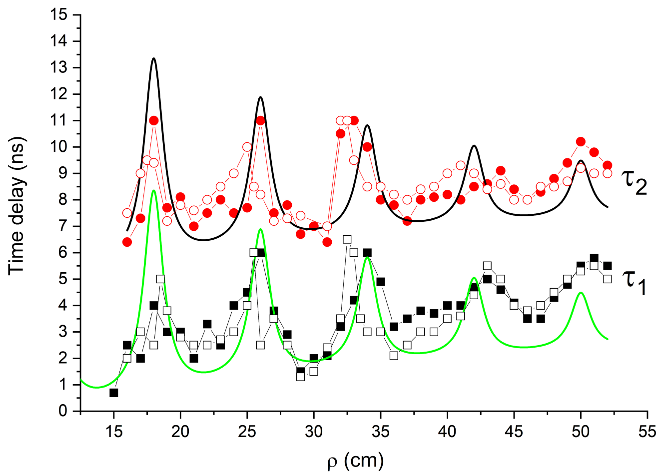

Figure 2. Two determinations of delay-time, relative to the rise time (τ_1) and the fall time (τ_2) of the square wave modulating the F_2 beam, measured for $\alpha \simeq 0°$, as a function of the distance ρ. The continuous lines were obtained using Equation (2) for parameter values as given in the text, the open symbols (circle and square) refer to the first determination, while the filled ones to the second.

The resulting spatial period can be interpreted, as anticipated above, assuming a competition (interference) of two waves forming an angle δ between their respective directions of propagation. For a given δ value, the dephasing between them, under the approximation of plane waves, will be given by $N(1-\cos\delta)/\cos\delta$, and in order to reobtain zero dephasing we need a number N of steps such that $N(1-\cos\delta)/\cos\delta \simeq 1$. This corresponds to a spatial period $\Delta\rho = N\lambda/2$, the factor $1/2$ being due to the plausible existence of standing wave behavior, so that the length of the steps to be considered is not λ but rather $\lambda/2$ [7], see Table 1.

Table 1. The spatial period ρ, corresponding to different values of δ, is reported for $\lambda = 3.226$ cm.

$\delta(°)$	$(1-\cos\delta)/\cos\delta$	$N(1-\cos\delta)/\cos\delta \simeq 1$ N	$\Delta\rho = N\lambda/2$ (cm)
42	0.346	3	4.84
38	0.269	4	6.45
34	0.206	5	8.07
32	0.179	6	9.68
25	0.103	10	16.13
20	0.064	16	25.81
15	0.035	30	48.35

From the data reported in Table 1, we have that the observed spatial period, $\Delta\rho \simeq 8$ cm of Figure 2, corresponds to an angle $\delta \simeq 34°$ between the direction of these waves. A more accurate and plausible interpretation will be given in Section 4.

In addition to the results reported in Figure 2, we have extended the delay-time measurements to the case in which a tilting angle α of the F_1 launcher was about $\pm 20°$, see Figures 3 and 4. The data there reported, even if comparable with those contained in Figure 2 obtained with $\alpha \simeq 0°$, exhibit a less regular behavior with respect to that of Figure 2, but the resulting spatial periodicity is certainly decidedly increased, up to 15–20 cm. This latter value can be attributed to values of δ of 20–25°, see Table 1. In Section 4, we will go into detail regarding this latter aspect.

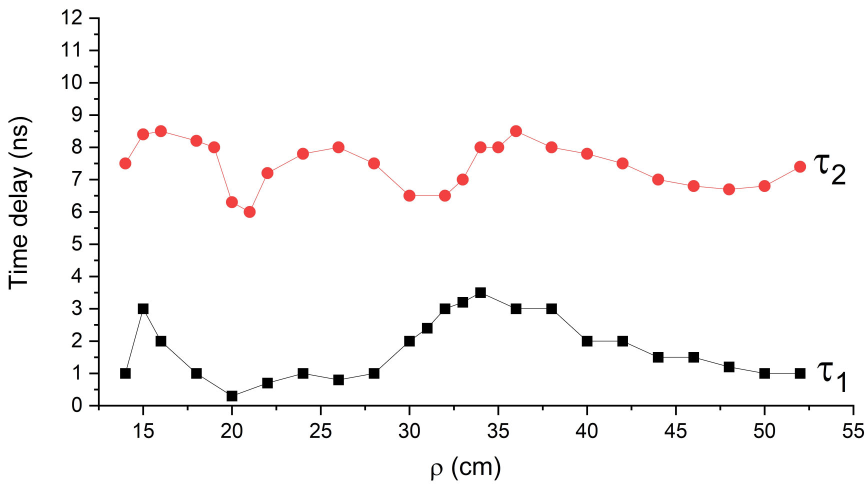

Figure 3. Same as Figure 2 for a tilting angle $\alpha \simeq 20°$, without fitting curve.

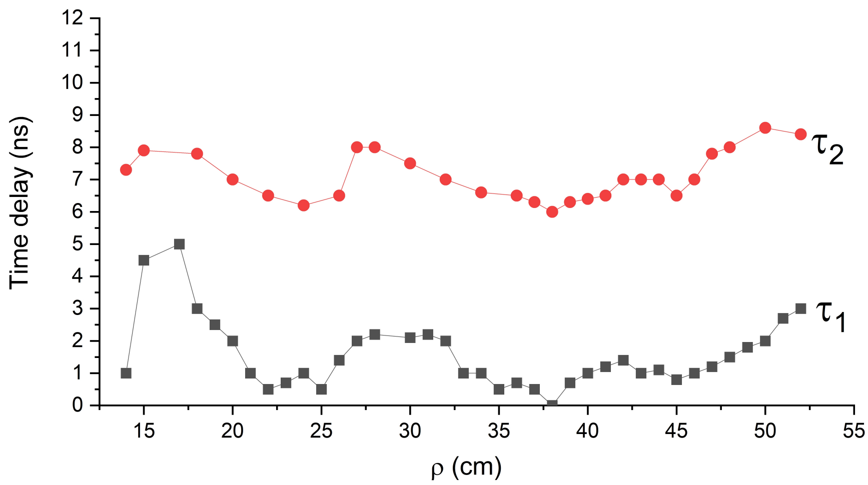

Figure 4. Same as Figure 3 for a tilting angle $\alpha \simeq -20°$.

4. Delay-Time Analysis

In this section, we will try to overcome the interpretation given in Section 3 for the delay-time results, providing a more convincing one. First, we have to note, as remarked since Ref. [1], that we are not dealing with long-range propagation but rather with a near-field situation.

Let us assume that the radiated field from the launcher F_1 can be expressed as that of a rectangular aperture having the dimensions of the mouth of the horn launcher, as schematically depicted in Figure 5. For simplicity, let us also assume the aperture dimensions as very large even along η ($d \gg \lambda$), that is, we assume the behavior to be independent on this coordinate; ξ, η, and ζ being the references axes with their origin O located in the center of the aperture. Under these assumptions, the field in the semi-space $\xi > 0$ can be expressed, in the scalar approximation, as a superposition of the plane waves in the form [8]

$$F(\xi, \zeta) = e^{-i\omega t} \int_{-\pi/2}^{+\pi/2} A(z) \exp[ik(\xi \cos z + \zeta \sin z)] dz, \tag{3}$$

where z is the angle (in the ζ, ξ plane) of the normal of the elementary wave with the ξ axis, $k = 2\pi/\lambda$ is the wave number, and $\omega = 2\pi\nu$ is the angular frequency.

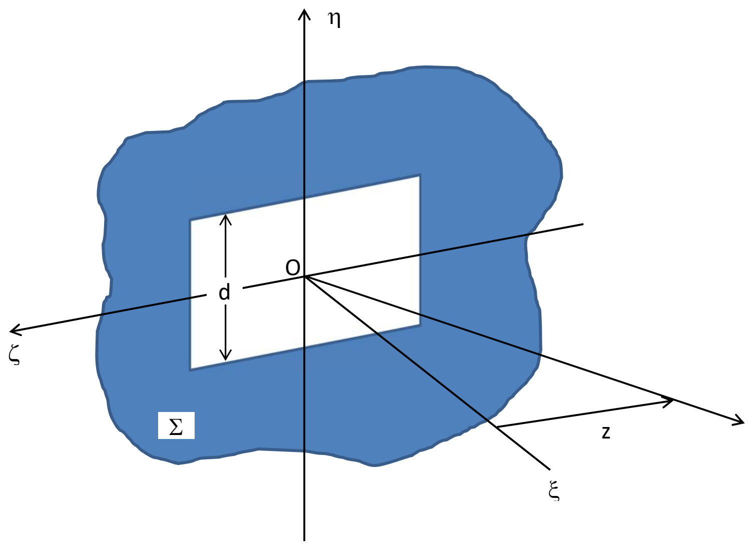

Figure 5. Schematic representation of the mouth of the F_1 horn launcher as an aperture in the Σ plane with the adopted coordinate axes.

In order to reproduce the field distribution in the Σ-plane of the aperture, we have to extend the limits of the integration of z in the complex plane by putting $z = x + iy$ and $\xi = \rho \cos \alpha$, $\zeta = \rho \sin \alpha$, ρ and α being the polar coordinates of the observation point, again in the ζ, ξ plane.

In consideration of this fact, and by substituting, the integral in Equation (3) becomes

$$\int_C A(z) \exp[ik(\rho \cos(z - \alpha))] dz, \tag{4}$$

where the integration path C is represented in Figure 6. For $\rho \gg \lambda$, we can evaluate the integral (4) in the saddle-point approximation. In this way, the original integration path C_0 is deformed in the steepest-descent path C, given by one branch of the equation $\cos(x - \alpha) \cosh y = 1$, which crosses the real axis at $z = \alpha$ with an angle equal to $-\pi/4$, see Figure 6.

In deforming the integration path, we have to consider the pole contribution if the amplitude $A(z)$ contains singularities in the region of the path-deformation.

Let us suppose that there are two poles at the complex points $\beta^{\pm} = \pm(\beta_r - i\beta_i)$. Depending on the α value, one or both poles can be captured by the deformed path. In the examples of Figure 6, with $\beta_r \simeq 30°$ and $\beta_i \simeq 10°$, we have that, for $\alpha = 20°$, only the pole at β^- is captured; analogously, for $\alpha = -20°$, only the pole at β^+ is captured; whereas, for $\alpha = 0°$, both poles at $\beta^{\pm}$ are captured.

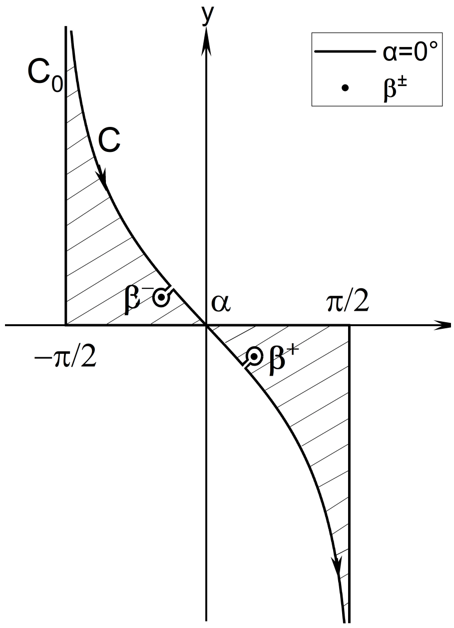

(**a**)

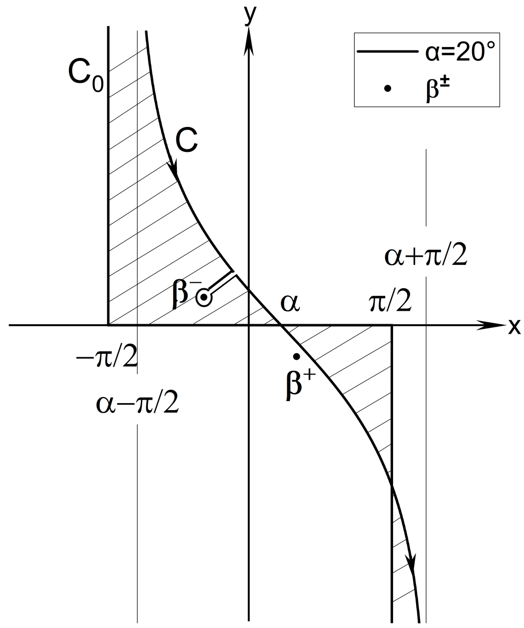

(**b**)

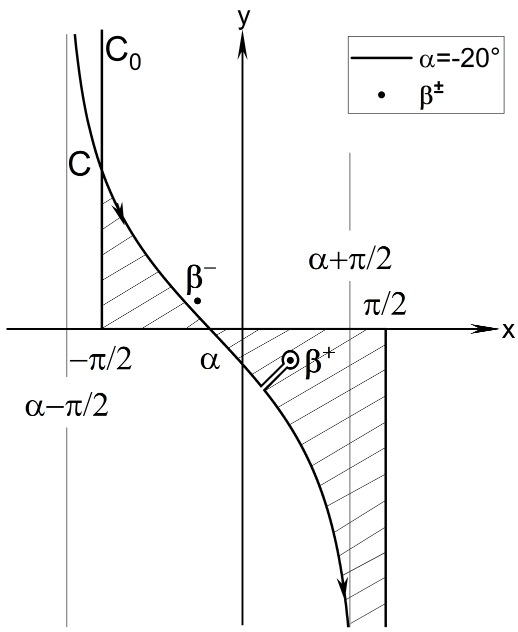

(**c**)

Figure 6. The original integration path C_0 is deformed into the steepest-descent path C taking into account the presence of pole singularities. In (**a**), case $\alpha \simeq 0°$, both the poles at $\beta^{\pm}$ are captured, and each one contributed as in (5). In (**b**), the case of $\alpha \simeq +20°$, only the pole at β^{-} is captured, while the one at β^{+} is not, but it contributes by Equation (7). In (**c**), case $\alpha \simeq -20°$, the pole at β^{+} is captured and β^{-} contributes by Equation (7). In the shaded areas, we have superluminal behavior.

When one pole is captured, the integral (4) can be expressed as

$$A(\alpha)\left(\frac{\lambda}{\rho}\right)^{1/2}\exp[i(k\rho-\pi/4)]+2\pi i\,\mathrm{res}[A(z\to\beta)]\exp[ik\rho\cos(\beta-\alpha)], \tag{5}$$

where the first term represents the normal (saddle-point) contribution: a cylindrical wave according to this unidimensional model; while the second one, due to the pole, represents a complex wave. Depending on the values of ρ and α, this second contribution can even prevail, in the near field, over the first one, especially when, according to the bidimensional model, the normal contribution becomes $A(\alpha)(\lambda/\rho)\exp[i(k\rho-\pi/2)]$. This latter properly represents a spherical wave that attenuated like λ/ρ and not like $(\lambda/\rho)^{1/2}$ as in (5) for the cylindrical wave [9].

By putting $\mathrm{res}[A(z\to\beta)]=\bar{A}(\beta)$ and recalling that $\beta=\beta_r-i\beta_i$, the contribution of the pole becomes:

$$2\pi i\bar{A}(\beta)\exp[ik\rho\cos(\beta_r-\alpha)\cosh\beta_i-k\rho\sin(\beta_r-\alpha)\sinh\beta_i]. \tag{6}$$

This represents a wave propagating in the β_r direction, with a velocity along a path with an angle α (phase-path velocity) given by $v_{pp}=c/(\cos(\beta_r-\alpha)\cosh\beta_i)$ where c is the light velocity in a vacuum, and that, depending on β and α, can be greater than c (superluminal behavior). Its amplitude attenuates with increasing α and ρ, while for $\beta_r\to\alpha$ and $\beta_i\to 0$, its contribution may be the dominant one in (5).

However, even if the pole is not captured by the steepest-descent path C, we still have a contribution that, according to Ref. [10], can be expressed, apart from the saddle-point contribution, as

$$I(\Omega)\simeq e^{i\Omega}\left[\pm i2\sqrt{\pi}e^{-\Omega b^2}Q(\mp ib\sqrt{\Omega})\right], \tag{7}$$

where $\Omega=k\rho$, $b=\{i[1-\cos(\beta-\alpha)]\}^{1/2}$, $\mathrm{Im}b\gtrless 0$, and $Q(y)=\int_y^\infty e^{-x^2}dx$ is the error function complement.

On the basis of the above considerations Equations (5)–(7), we can better explain the results reported in Figures 2–4. When the tilting angle of the launcher F_1 is nearly zero ($\alpha\simeq 0$, in the case of Figure 2), the more probable situation of the integration path is the one represented in Figure 6a. In this case in order to reproduce the spatial periodicity $\Delta\rho\simeq 8$ cm of Figure 2, both poles at $\pm\beta$ are captured, with values of $\pm\beta_r$ nearly coincident with $\delta\simeq 34^\circ$. The two involved waves are those of Equation (5), the periodicity of the amplitude is the one in (6), given by $\cos(\beta_r-\alpha)\cosh\beta_i$, with $\beta_r-\alpha\simeq\delta$ and $\cosh\beta_i\simeq 1$. This, in turn, causes the periodicity in $\tau(\rho)$, Equation (2), analogously to what is shown in the case of Ref. [6].

In the cases of tilting angles $\alpha\simeq\pm 20^\circ$ (Figures 3 and 4), the situation is different, as shown in Figure 6b,c. There, we have that only one pole, β^- for $\alpha\simeq 20^\circ$, is captured while β^+ is not, but it is located near the saddle-point, so that its contribution, according to Equation (7), may be the prevalent one causing a periodicity, determined by b^2 in Equation (7), that is, by $\beta_r^+-\alpha\simeq 34^\circ-20^\circ=14^\circ$, a value that, according to Table 1, would produce a periodicity exaggerated to a size of $\simeq$37 cm, while the value resulting from Figures 3 and 4, as previously noted, is about 15–20 cm.

However, we have to remark that the contribution due to the captured pole β^-, although presumably of minor importance due to the distance from the saddle-point with $\beta_r^-+\alpha=54^\circ$, would produce a periodicity of less than 4 cm. This latter was not evidenced in the experiments (Figures 3 and 4), but it is reasonable to assume it may influence the observation. For $\alpha=-20^\circ$, the situation is similar to the role of the inverted poles.

5. Concluding Remarks

On the basis of the results reported above, along with their interpretation, it can be safely concluded that the observed behavior, i.e., the angular dependence of the time delay, confirms the assumptions made about the theoretical modeling adopted. As for the resulting values of $\beta_r = \pm 34^\circ$, we note that they are comparable with those obtained in single beam experiments, see f.i. Figure 7 contained in Ref. [8] where β_r resulted to be $\pm 27^\circ$.

As for the origin of the transfer of modulation between the two beams, the hypothesis made in Ref. [1] is still tenable, once demonstrated that the cross-talking between F_1 and F_2 launchers is indeed negligible. In fact, the ratio S/S_R of the intensities, relative to the signal S and to the residuals S_R, turned out to be of the order of 10^2, a value that makes the S_R contribution, even if still present, of secondary importance [11].

In particular, as recalled in the Introduction, the modulation transfer has been hypothesized as due to a photon–photon scattering mechanism occurring in the presence of a stochastic process. Arguments in favor of this assumption have been given in [1] on the basis of relativistic considerations [12], see also references [13–17] for related topics.

Author Contributions: Conceptualization, I.C. and A.R.; Methodology, I.C. and A.R.; Investigation, I.C. and A.R.; Writing—original draft, I.C. and A.R.; Writing—review & editing, I.C. and A.R. All authors have read and agreed to the published version of the manuscript.

Funding: This research received no external funding.

Data Availability Statement: The data that support the findings of this study are available from the corresponding author upon reasonable request.

Conflicts of Interest: The authors declare no conflict of interest.

References

1. Ranfagni, A.; Cacciari, I. Modulation Transfer between Microwave Beams: A Hypothesized Case of a Classically-Forbidden Stochastic Process. *Axioms* **2022**, *11*, 416. [CrossRef]
2. Cacciari, I.; Mugnai, D.; Ranfagni, A.; Petrucci, A. Cross-modulation between microwave beams interpreted as a stochastic process. *Int. J. Mod. Phys. B* **2021**, *35*, 2150037. [CrossRef]
3. Cacciari, I.; Mugnai, D.; Ranfagni, A. Delay time in the tansfer of modulation between between microwave beams. *Eng. Rep.* **2021**, *3*, e12392.
4. Kac, M. A Stochastic Model Related to the Telegrapher's Equation. *Rocky Mountain J. Math.* **1974**, *4*, 497–509. [CrossRef]
5. DeWitt-Morette, C.; Foong, S.K. Path-integral solutions of wave equations with dissipation. *Phys. Rev. Lett.* **1989**, *62*, 2001–2004. [CrossRef] [PubMed]
6. Mugnai, D.; Ranfagni, A. Microwave propagation of surface waves. *Opt. Commun.* **2014**, *313*, 22–26. [CrossRef]
7. Terman, T.E. *Electronic and Radio Engineering*; McGraw-Hill: New York, NY, USA, 1955; Chapter 4.
8. Ranfagni, A.; Fabeni, P.; Pazzi, G.P.; Mugnai, D. Anomalous pulse delay in microwave propagation: A plausible connection to the tunneling time. *Phys. Rev. E* **1993**, *48*, 1453–1460. [CrossRef] [PubMed]
9. Ranfagni, A.; Agresti, A.; Cacciari, I. Angular dependence in anomalous microwave propagation: A bidimensional treatment. *J. Appl. Phys.* **2014**, *115*, 104902. [CrossRef]
10. Felsen, L.B.; Marcovitz, N. *Radiation and Scattering of Waves*; Prentice Hall: Englewood Cliffs, NJ, USA, 1973; Chapter 4.
11. Cacciari, I.; Ranfagni, A. On the origin of the transfer of modulation between microwave beams. *Mod. Phys. Lett. B* **2022**, *36*, 2250096. [CrossRef]
12. Toraldo di Francia, G. *L'indagine del Mondo Fisico*; Giulio Einaudi: Torino, Italy, 1976; p. 338.
13. Radice, M. One-dimensionale telegraphic process with noninstantaneous stochastic resetting. *Phys. Rev. E* **2021**, *104*, 044126. [CrossRef] [PubMed]
14. Giona, M.; Cairoli, A.; Klages, R. Extended Poisson-Kac theory: A unifying framework for stochastic processes with finite propagation velocity. *Phys. Rev. X* **2022**, *2*, 021004. [CrossRef]
15. Luo J.; Tu, L.C.; Hu, Z.K.; Luan, E.J. New Experimental Limit on the Photon Rest Mass with a Rotating Torsion Balance. *Phys. Rev. Lett.* **2003**, *90*, 081801. [CrossRef] [PubMed]
16. Jacobson, T.; Schulman, L.S. Quantum stochastics: The passage from a relativistic to a non-relativistic path integral. *J. Phys. A* **1984**, *17*, 375–383. [CrossRef]
17. Feynman, E.R.P.; Hibbs, A.R. *Quantum Mechanics and Path Integrals*; McGraw-Hill: New York, NY, USA, 1965; Chapter 7.